

# Probing the homogeneous spectral function of a trapped atomic Fermi gas using momentum resolved rf spectroscopy

Qijin Chen

*Department of Physics and Zhejiang Institute of Modern Physics,  
Zhejiang University, Hangzhou, Zhejiang 310027, CHINA*

(Dated: December 2, 2024)

Momentum resolved rf spectroscopy has been demonstrated to be able to probe the averaged spectral function in a Fermi gas. However, the usefulness of this technique was limited by the inhomogeneity across the trap. Here we propose that using phase separation at high population imbalances at low temperature, one can essentially extract the centrally important spectral function of a homogeneous Fermi gas (at the trap center) with momentum resolved rf spectroscopy. We present theoretically calculated spectral functions and spectral intensity maps for various cases over the entire BCS-BEC crossover to support this proposal.

PACS numbers: 03.75.Hh, 03.75.Ss, 74.20.-z

Ultracold atomic Fermi gases has emerged as a rapidly developing field, bridging condensed matter and atomic and optical physics. Using a Feshbach resonance, the effective two-body interaction can be easily tuned from weak to strong, effecting a BCS–Bose-Einstein condensation (BEC) crossover phenomenon, with an applied detuning magnetic field. At the same time, the population imbalance can also be readily varied experimentally. Due to these easy tunability of system parameters, atomic Fermi gases can be viewed as quantum simulators of many important condensed matter systems, such as the Hubbard model and high  $T_c$  superconductors [1, 2].

Of central importance in a many-body system is the fermionic spectral function  $A(\mathbf{k}, \omega)$ . Once  $A(\mathbf{k}, \omega)$  is known, it can be used to calculate essentially all other physical quantities. Due to the extremely small size of a Fermi gas cloud and its charge neutrality, it is hard to apply conventional experimental techniques from condensed matter to atomic Fermi gases. Measurements often involves integration of the entire momentum space and the entire trap. The intrinsic spatial inhomogeneity introduced by the trapping potential constitutes another severe problem to this end. It has been a long-sought goal to be able to extract the homogeneous properties, esp.  $A(\mathbf{k}, \omega)$ , from measurements in the trap.

In this Letter, we propose that one can use momentum resolved rf spectroscopy in conjunction with a high population imbalance to measure the homogeneous spectral function  $A(\mathbf{k}, \omega)$  corresponding to the density and chemical potential at the trap center.

Since the first experimental realization of BCS-BEC crossover, many different measurements have been done on atomic Fermi gases, including thermodynamic and transport measurements, as well as collective excitations, etc. Among all these measurements, the most direct probe of the single particle properties is arguably the radio-frequency (rf) spectroscopy. The first generation of rf measurements involves integration over the entire trap and the whole momentum space. This led to a two-peak structure of the rf spectra at an intermediate temperature below  $T_c$ . Due to the integrations, controversies arose regarding the theoretical interpretation of the

origin of this two-peak structure. Final state effects in  $^6\text{Li}$  further complicated this matter.

Tomographic rf spectroscopy was developed by the MIT group [3], which provides a measurement of the local rf spectrum. While this technique has spatial resolution, however, it involves integration over the entire momentum space, and therefore cannot be used as a probe of the spectral function  $A(\mathbf{k}, \omega)$ .

Recently, Ho and Zhou [4] proposed a theoretical scheme which allows one to calculate the density and fermionic chemical potential  $\mu$  at the trap center or as a function of the radius  $r$ . However, this procedure relies on the assumption of a strict harmonic trapping potential,  $V_{trap} = \frac{1}{2}m(\omega_x^2 x^2 + \omega_y^2 y^2 + \omega_z^2 z^2)$ . Unfortunately, this is often not satisfied, since the real trap potential is usually of a gaussian form,  $V_{trap}(r) = V_0[1 - e^{-m\bar{\omega}^2 r^2/2V_0}]$ , which can be approximated by a parabolic potential only at very low temperature and with a high trap depth, where  $\bar{\omega}$  is the average trap frequency. For example, in comparison with the counterpart in a harmonic trap, for a realistic trap depth  $V_0/E_F^0 = 10$  and 6.67 ( $\gg 1$ ), the calculated entropy is 10.35% and 20.6% higher and the energy is 13.0% and 25.6% higher, respectively, where  $E_F^0 \equiv k_B T_F^0 \equiv \hbar^2(k_F^0)^2/2m$  and  $k_F^0$  are the global Fermi energy and Fermi momentum in the noninteracting limit (for the majority atoms in the population imbalanced case). Therefore, the Ho-Zhou scheme cannot be applied in a realistic situation. Furthermore, this scheme does not provide any information regarding the microscopics such as the spectral function.

The controversies regarding the origin of the aforementioned double peak structure have largely been cleared by the recent experiments [5] on  $^{40}\text{K}$ , near or slightly above  $T_c$ , using momentum resolved rf spectroscopy. With momentum resolution, the rf spectroscopy essentially measures the fermionic spectral function  $A(\mathbf{k}, \omega)$ , which is of central importance in a many-body system. It is the atomic gas counterpart of the angle resolved photoemission spectroscopy (ARPES) [6] for a traditional condensed matter system. However, this is true only for a homogeneous Fermi gas. Although, as we have shown previously, in the trap the momentum resolved rf spec-

troscopy can provide useful information about  $A(\mathbf{k}, \omega)$ , the inherent spatial inhomogeneity severely limits the quantitative resolution of the extracted spectral function in the experiment of Ref. [5], which involves integration over the entire trap.

It is the purpose of the present Letter to address this inhomogeneity issue and propose that it can be largely avoided utilizing phase separation at high population imbalances. Although throughout this paper we will use a particular pairing fluctuation theory to do computations, we emphasize that the proposal itself is model independent and can be applied in other theories as well.

As mentioned elsewhere [7], the use of  $^{40}\text{K}$  rather than  $^6\text{Li}$  is crucial in extracting  $A(\mathbf{k}, \omega)$ , since there are no complications from final state interactions [8–11] near the usual Feshbach resonance around 202 G, unlike the case with the 834 G resonance of  $^6\text{Li}$ . It is for this reason that the rf spectral intensity for  $^{40}\text{K}$  is simply proportional to the spectral function  $A(\mathbf{k}, \omega)$ . For  $^6\text{Li}$ , extra efforts are needed in order to extract  $A(\mathbf{k}, \omega)$  from the rf spectral intensity measurements.

The spectral function  $A(\mathbf{k}, \omega)$  can be used to uniquely construct the Green's function and the single particle self energy, for which different theories often give different results. Therefore, the more accurate the measurement of  $A(\mathbf{k}, \omega)$ , the easier it is to test different theories. For example, a comparison [12, 13] of different BCS-BEC crossover approaches suggested important differences in the dispersive behavior of  $A(\mathbf{k}, \omega)$ . The theoretical scheme we use in this paper exhibit a clear and robust downward dispersion [7] in the spectral intensity plot near  $T_c$ , manifesting an existing pseudogap before the onset of superfluidity at lower  $T = T_c$ , different from the alternative scheme [14, 15] which follows the approach of Nozières and Schmitt-Rink (NSR) [16]. A quantitatively accurate measurement of  $A(\mathbf{k}, \omega)$  should serve to unambiguously test these two schools of theories.

We now recapitulate the physics underlying typical rf spectroscopic measurements. Pairing takes place between the 1-2 hyperfine states. An rf field of frequency  $\nu$  is used to excite the atoms in hyperfine level 2 to another internal state, i.e., level 3. For  $^{40}\text{K}$ , atoms in level 3 do not interact with those in level 1 and thus can be regarded as free, non-interacting atoms. Since the momentum of the rf photon is negligible, the momentum distribution of level 3 atoms reflects that of level 2 atoms, and can be measured using the time of flight technique following a ballistic expansion of the Fermi gas. In a population imbalanced case, one can choose the minority to be level 2 atoms, as we do here.

The rf current for transitions of atoms from level 2 to level 3 can be calculated using the linear response theory in a many-body theoretical language, and is reduced to the computation of the retarded correlation function  $\langle G(K)G_3^{(0)}(K+Q) \rangle$ , where  $G(K)$  is the Green's function for level 2 atoms, and  $G_3^{(0)}$  for the (noninteracting) level 3 atoms. Here  $K \equiv (i\omega_l, \mathbf{k})$  and  $Q \equiv (i\Omega_n, \mathbf{q})$ , where  $\omega_l$  and  $\Omega_n$  are odd and even Matsubara frequencies, respectively. For rf photos,  $\mathbf{q} = 0$ . Since  $G_3^{(0)}$  is noninteracting, as has been derived previously

[7, 17], we have for the momentum-resolved RF current

$$I(\mathbf{k}, \delta\nu) = \frac{1}{2\pi} A(\mathbf{k}, \omega) f(\omega) \Big|_{\omega=\xi_{\mathbf{k}}-\delta\nu}, \quad (1)$$

where  $A(\mathbf{k}, \omega) = -2 \text{Im} G(\mathbf{k}, \omega + i0)$  is the spectral function,  $f(x)$  the Fermi distribution function, and we have take the transition matrix element to be a constant and set to unity. It is evident that this is very similar to ARPES, which measures  $A(\mathbf{k}, \omega)$  in a conventional condensed matter system. Note that here  $\delta\nu = h\nu - \Omega_L$  is the rf detuning, where  $\nu$  is the rf photon frequency,  $\Omega_L$  the energy splitting between electronic level 2 and level 3. The frequency  $\omega = \xi_{\mathbf{k}} - \delta\nu$  corresponds to the energy of state 2 measured with respect to the Fermi level, where  $\xi_{\mathbf{k}} = k^2/2m - \mu$ ,  $\mu$  is the chemical potential of atoms in state 2. We take  $\hbar = 1$ . It is obvious that when level 2 atoms are free, we have  $\delta\nu = 0$  and  $\omega = \xi_{\mathbf{k}}$ ; the former gives the sharp peak at zero detuning as shown in previous rf spectroscopy data [18] whereas the latter gives the free electron dispersion in the spectral intensity map in the  $\omega - k$  plane in Ref. 5. As has been used in the experiment[5], the angle-integrated ‘‘occupied spectral intensity’’ is given by  $I^{photo}(k, \omega) \equiv (k^2/2\pi^2)A(k, \omega)f(\omega)$ .

The central issue here is to calculate the spectral function or equivalently the Green's function  $G(K)$  for minority (level 2) atoms. In the presence of population imbalance, detailed calculation of the superfluid phase diagram, the Green's function and density profiles in each phase can be found in Refs. 19–22. In the case of phase separation in a trap, as shown in Fig. 2 of Ref. [19], there is a BCS superfluid core (without population imbalance), surrounded by the majority atoms. To a first order approximation, the density profile of the minority atoms can be approximated by truncating a density profile of an unimbalanced Fermi gas at the (sharp) phase separation boundary.

With and without population imbalance, the normal state self energy  $\Sigma_{pg}$  follow a rather simple BCS-like form [7, 12, 23] in the context of both atomic Fermi gases [17, 24] and the cuprate superconductors [2, 6, 25]. Following our previous body of work [7, 17, 23], in the superfluid state, for atomic Fermi gases, the self energy  $\Sigma(K)$  contains two terms, associated with the condensed ( $\Sigma_{sc}$ ) and noncondensed fermion pairs ( $\Sigma_{pg}$ ), respectively:  $\Sigma(\mathbf{k}, \omega) = \Sigma_{pg}(\mathbf{k}, \omega) + \Sigma_{sc}(\mathbf{k}, \omega)$ , where

$$\Sigma_{pg}(\mathbf{k}, \omega) = \frac{\Delta_{pg}^2}{\omega + \xi_{\mathbf{k}} + i\gamma} - i\Sigma_0, \quad \Sigma_{sc}(\mathbf{k}, \omega) = \frac{\Delta_{sc}^2}{\omega + \xi_{\mathbf{k}}}.$$

Here the broadening  $\gamma \neq 0$  and ‘‘incoherent’’ background contribution  $\Sigma_0$  can be determined by fitting the experimentally measured rf spectra. The precise values of  $\gamma$  and  $\Sigma_0$ , and their  $T$ -dependencies are not particularly important for the present purposes. As in Ref. [7], here we will take  $\Sigma_0$  as temperature independent,  $\gamma$  linear in  $T/T_c$ . Both scale with local  $E_F(r)$ . The rf spectra are finally convoluted with a Gaussian broadening function with a standard deviation  $\sigma$ , reflecting the instrumental resolution in experiment.

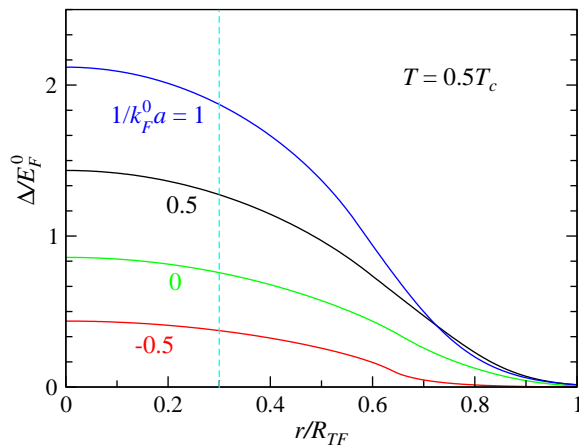


Figure 1. (Color online) Radial profile of the excitation gap  $\Delta/E_F^0$  in the superfluid phase of a trapped Fermi gas without population imbalance for  $1/k_F^0 a = -0.5, 0, 0.5$  and  $1$ , corresponding to BCS through BEC regimes, calculated at  $T = 0.5T_c$ . The gap is nearly flat for  $r < 0.3R_{TF}$ .

We first study the radial profile of the excitation gap of a trapped atomic Fermi gas in the superfluid phase, as shown in Fig. 1. It suffices to calculate for the cases in the absence of a population imbalance, since in the presence of phase separation which is of primary interest in the present study, different population imbalances can be regarded as the curves in Fig. 1 cut off at different radii. For simplicity, here the data were all calculated at  $T = 0.5T_c$ . From the bottom to the top, the curves correspond to  $1/k_F^0 a = -0.5$  (BCS case),  $0$  (unitary),  $0.5$  (pseudogap) and  $1.0$  (BEC) cases, respectively, where  $a$  the inter-fermion  $s$ -wave scattering length. From Fig. 1, we conclude that for radius  $r < 0.3R_{TF}$ , the gap is nearly flat from BCS through BEC regimes, where  $R_{TF} = \sqrt{2E_F^0/m\bar{\omega}^2}$  is the Thomas-Fermi radius.

With this knowledge, now we study the occupied spectral intensity maps of the minority (spin down) atoms in the  $(\omega + \mu(r)) - k$  plane for different degrees of population imbalance, as characterized by the size of the radius  $R_\downarrow$  of the minority atomic gas. For illustration purpose, we present the result for the unitary case in a harmonic trap with phase separation in Fig. 2, for (a)  $R_\downarrow = 0.1R_{TF}$ , (b)  $0.2R_{TF}$ , (c)  $0.3R_{TF}$ , and (d)  $0.4R_{TF}$ , respectively. Note here that, as in Ref. [7], we use  $\omega + \mu(r)$  instead of  $\omega$  in the vertical axis, since the former is constant for given  $k$  across the trap, representing the single particle energy measured from the bottom of the band. While Fig. 2(a) corresponds to an extremely high population imbalance, which may not be readily realizable experimentally, Fig. 2(c)-(d) certainly falls in the experimentally accessible range. The (magenta) dashed curves represent the local (or homogeneous) dispersion at the trap center, and the (white) solid curves are the quasiparticle dispersion given by the loci of the peak location of the energy distribution curves (EDC). It is evident that up to  $R_\downarrow = 0.4R_{TF}$ , the two sets of curves are essentially indistinguishable.

Next we study whether the same conclusion holds for the

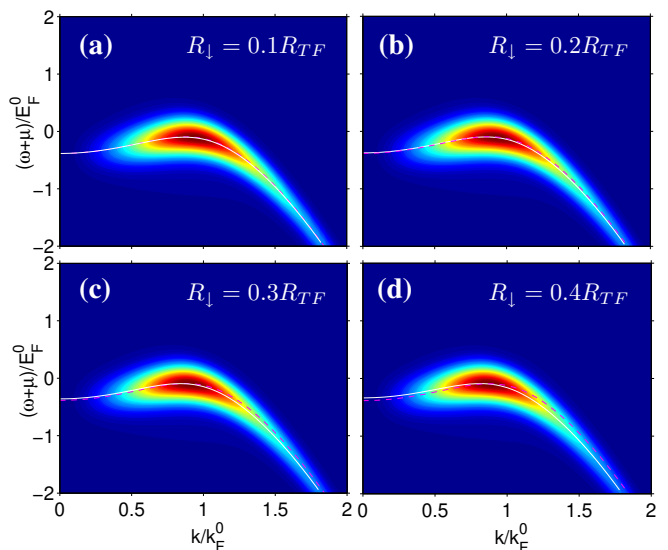


Figure 2. (Color online) Occupied spectral intensity maps  $I^{photo}(k, \omega)$  for the minority atoms of a population imbalanced, phase separated unitary Fermi gas in a harmonic trap for (a)  $R_\downarrow = 0.1R_{TF}$ , (b)  $0.2R_{TF}$ , (c)  $0.3R_{TF}$ , and (d)  $0.4R_{TF}$ , respectively, calculated at  $T = 0.13T_F^0$ . The (magenta) dashed curves represent the local (or homogeneous) dispersion at the trap center, and the (white) solid curves are the quasiparticle dispersion given by the loci of the peak location of the EDC. In order to maximize the splitting between the two curves, here we take relatively small broadening,  $\Sigma_0 = \gamma(T_c) = 0.1E_F^0$  at the trap center. The rf spectra were convoluted with an instrumental Gaussian broadening function with a standard deviation  $\sigma = 0.2E_F^0$  (as appropriate for experiment in Ref. [5]). It is evident that up to  $R_\downarrow = 0.4R_{TF}$ , the two sets of curves are essentially indistinguishable.

entire BCS-BEC crossover. Shown in Fig. 3 are the occupied spectral intensity maps of the minority atoms of population imbalanced, phase separated atomic Fermi gases in a harmonic trap with minority radius  $R_\downarrow = 0.3R_{TF}$  for (a)  $1/k_F^0 a = -0.5$  (BCS case), (b)  $0$  (unitary), (c)  $0.5$  (pseudogap), and (d)  $1.0$  (BEC case), calculated at  $T = 0.09T_F^0$ ,  $0.13T_F^0$ ,  $0.15T_F^0$  and  $0.15T_F^0$ , respectively ( $0.5T_c$  for each case). Since the atomic cloud shrinks with increasing  $1/k_F^0 a$ , these same  $R_\downarrow$  corresponds to a population imbalance of about  $p \equiv (N_\uparrow - N_\downarrow)/(N_\uparrow + N_\downarrow) = 0.9 \sim 0.7$ . Here the broadening parameters  $\gamma$  and  $\Sigma_0$  increase from BCS to BEC, reflecting an increasing excitation gap. Clearly, for all cases from BCS through BEC regimes, the dispersion extracted from the trap averaged minority atoms are very close to that calculated at the trap center.

Note that the up-curving branch of the dispersion of thermally excited quasiparticles is completely suppressed by  $f(\omega)$  and becomes invisible here. However, its leftover at large  $k$  form a very weak and broad peaks at negative  $\omega$ , as indicated by the light blue area above the downward dispersion branch. At higher  $T$ , this feature [26] naturally explains the abrupt jump in the quasiparticle dispersions extracted at higher  $T$  using a single peak fit in Fig. 1 of Ref. [27].

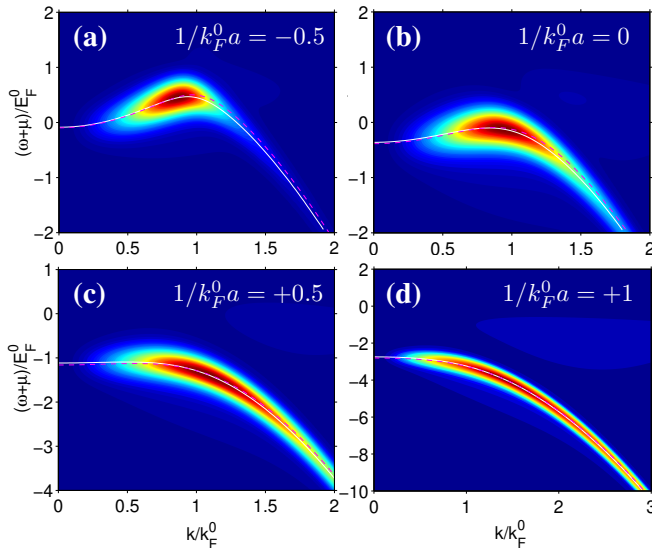


Figure 3. (Color online) Occupied spectral intensity maps  $I^{photo}(k, \omega)$  for the minority atoms of a population imbalanced, phase separated Fermi gas with  $R_{\downarrow} = 0.3R_{TF}$  for (a)  $1/k_F^0 a = -0.5$  (BCS case), (b) 0 (unitary), (c) 0.5 (pseudogap), and (d) 1.0 (BEC case), respectively. They are calculated at  $T = 0.5T_c$  or  $T = 0.09T_F^0$ ,  $0.13T_F^0$ ,  $0.15T_F^0$  and  $0.15T_F^0$ , respectively. The (magenta) dashed curves represent the local (or homogeneous) dispersion at the trap center, and the (white) solid curves are the quasiparticle dispersion given by the loci of the peak location of the EDC. The parameters  $\Sigma_0 = \gamma(T_c)$  at the trap center are (a)  $0.1E_F^0$ , (b)-(c)  $0.2E_F^0$ , and (d)  $0.35E_F^0$ , respectively. The instrumental broadening  $\sigma = 0.2E_F^0$ . For all cases, the two sets of curves are essentially indistinguishable.

Finally, in Fig. 4, we present a direct comparison of the (occupied) spectral function between (a,b) the atoms at the trap center and (c,d) the trap averaged minority atoms of a highly population imbalanced, phase separated Fermi gas. The curves are for momentum  $k = 0.88k_F^0 \approx \sqrt{2m\mu}(r=0)$ , which is near the Fermi level [where  $A(k, \omega)$  is most sensitive to the variation of  $\Delta$ ] at the trap center. The spectral peaks at  $+E_{\mathbf{k}} \approx \Delta$  are suppressed by  $f(\omega)$ . The narrow peaks (a) and (c) are the spectral lines without instrumental broadening, and the broad ones (b) and (d) are the same result but convoluted with instrumental broadening. In particular, line (d) corresponds to the vertical cut (EDC) at  $k = 0.88k_F^0$  in Fig. 1(c) but without the  $k^2/2\pi^2$  factor, replotted as a function of  $\omega$ . There are small differences between the unconvoluted spectral peaks (a) and (c) in the peak location and peak height (or equivalently peak width). This is primarily due to the gradually decreasing broadening parameters caused by decreasing local Fermi energy  $E_F(r)$  as  $r$  increases, leading to slightly higher peak and smaller average gap (given by the peak location). We emphasize that these differences are barely discernible and are completely washed out by instrumental broadening, as revealed by the complete overlap between lines (b) and (d). The complete spectral function  $A(k, \omega)$  can be obtained by dividing the unconvoluted lines (a,c) by  $f(\omega)$ .

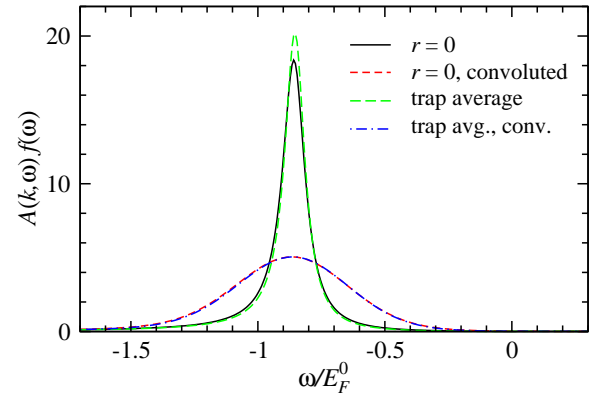


Figure 4. (Color online) Comparison of occupied spectral function  $A(k, \omega)f(\omega)$  between (a)-(b) atoms at the trap center and (c)-(d) trap averaged minority atoms, for a population imbalanced, phase separated unitary Fermi gas with  $R_{\downarrow} = 0.3R_{TF}$  at  $T = 0.5T_c = 0.13T_F^0$ . The spectra are calculated for  $k = 0.88k_F^0 \approx \sqrt{2m\mu}(r=0)$  near the Fermi surface. The narrow peaks (a) and (c) are the intrinsic spectral line, whereas the broad ones (b) and (d) are those convoluted with a instrumental broadening function. The broadening parameters  $\Sigma_0$ ,  $\gamma$  and  $\sigma$  are the same as in Fig. 1. The trap averaged minority spectral function is nearly the same as that at the trap center.

In conclusion, Figs. 1-4 demonstrate that in the presence of phase separation for a highly population imbalanced Fermi gas, the trap averaged quasiparticle dispersion of the minority atoms is very close to that at the trap center. Therefore, one can use the former dispersion to essentially extract not only the excitation gap and the fermionic chemical potential but also the complete spectral function at the trap center. This scheme does not depend on our particular BCS-BEC theory, nor does it depend on the strict harmonicity of the trapping potential. As long as phase separation can occur, one can use this scheme to extract  $A(k, \omega)$  at the trap center. For higher  $T$  where phase separation is prohibited, one may combine a narrow imaging laser beam with appropriate population imbalance in the Sarma or breached pair state [19] to achieve similar results. Details require further study.

This work is supported by NSF of China (grant No. 10974173) and by the Cheung Kong Scholars Programme of China, by MOST of China (grant No. 2011CB921300), by the Fundamental Research Funds for the Central Universities of China (Program No. 2010QNA3026), and by Zhejiang University (grant No. 2009QNA3015).

- 
- [1] A. J. Leggett, Nat. Phys., **2**, 134 (2006).
  - [2] Q. J. Chen, J. Stajic, S. N. Tan, and K. Levin, Phys. Rep., **412**, 1 (2005).
  - [3] Y. Shin, C. H. Schunck, A. Schirotzek, and W. Ketterle, Phys. Rev. Lett., **99**, 090403 (2007).
  - [4] T.-L. Ho and Q. Zhou, Nat. Phys., **6**, 131 (2009).
  - [5] J. T. Stewart, J. P. Gaebler, and D. S. Jin, Nature (London), **454**,

- 744 (2008).
- [6] A. Kanigel *et al.*, Phys. Rev. Lett., **101**, 137002 (2008).
- [7] Q. J. Chen and K. Levin, Phys. Rev. Lett., **102**, 190402 (2009).
- [8] A. Perali, P. Pieri, and G. C. Strinati, Phys. Rev. Lett. **100**, 010402 (2008); M. Punk and W. Zwirger, *ibid.* **99**, 170404 (2007); Z. Yu and G. Baym, Phys. Rev. A **73**, 063601 (2006).
- [9] S. Basu and E. Mueller, Phys. Rev. Lett., **101**, 060405 (2008).
- [10] Y. He, C. C. Chien, Q. J. Chen, and K. Levin, Phys. Rev. Lett., **102**, 020402 (2009).
- [11] Q. J. Chen, Y. He, C.-C. Chien, and K. Levin, Rep. Prog. Phys., **72**, 122501 (2009).
- [12] J. Maly, B. Jankó, and K. Levin, Physica C **321**, 113 (1999); Phys. Rev. B **59**, 1354 (1999).
- [13] K. Levin, Q. J. Chen, Y. He, and C.-C. Chien, Ann. Phys., **325**, 233 (2010).
- [14] A. Perali, P. Pieri, G. C. Strinati, and C. Castellani, Phys. Rev. B, **66**, 024510 (2002).
- [15] P. Massignan, G. M. Bruun, and H. T. C. Stoof, Phys. Rev. A, **77**, 031601(R) (2008).
- [16] P. Nozières and S. Schmitt-Rink, J. Low Temp. Phys., **59**, 195 (1985).
- [17] Y. He, Q. J. Chen, and K. Levin, Phys. Rev. A, **72**, 011602(R) (2005).
- [18] C. Chin, M. Bartenstein, A. Altmeyer, S. Riedl, S. Jochim, J. Hecker-Denschlag, and R. Grimm, Science, **305**, 1128 (2004).
- [19] C.-C. Chien, Q. J. Chen, Y. He, and K. Levin, Phys. Rev. Lett., **98**, 110404 (2007).
- [20] Y. He, C.-C. Chien, Q. J. Chen, and K. Levin, Phys. Rev. A, **75**, 021602(R) (2007).
- [21] Q. J. Chen, H. Yan, C.-C. Chien, and K. Levin, Phys. Rev. B, **75**, 014521 (2007).
- [22] Y. He, C.-C. Chien, Q. J. Chen, and K. Levin, Phys. Rev. B, **76**, 224516 (2007).
- [23] Q. J. Chen, K. Levin, and I. Kosztin, Phys. Rev. B, **63**, 184519 (2001).
- [24] J. Kinnunen, M. Rodriguez, and P. Törmä, Science **305**, 1131 (2004); Phys. Rev. Lett. **92**, 230403 (2004).
- [25] Q. J. Chen and K. Levin, Phys. Rev. B, **78**, 020513(R) (2008).
- [26] Q. J. Chen, Talk A16.00005, the American Physical Society March Meeting, Pittsburgh, PA, USA, 2009.
- [27] J. P. Gaebler, J. T. Stewart, T. E. Drake, D. S. Jin, A. Perali, P. Pieri, and G. C. Strinati, Nat. Phys., **6**, 569 (2010).